Application of the Unified CPT method to assess the driving resistance of pipe piles in sand

Barry Lehane [i], David Igoe [ii], Kenneth Gavin [iii] and Eduardo Bittar[iv]

i) Professor, Department of Civil Engineering, University of Western Australia

ii) Asst. Professor, Department of Civil Engineering, Trinity College Dublin, Ireland.

iii) Professor, Department of Civil Engineering , TUDelft, The Netherlands

iv) PhD student, Department of Civil Engineering, University of Western Australia

ABSTRACT

A new method of estimating the static capacity of driven piles in silica sand, referred to as the Unified method, is included in the forthcoming 2022 edition of ISO-19901-4 and replaces the four CPT methods recommended in ISO-19901-4 (2016). This paper investigates the application of this method to the prediction of driving resistance of pipe piles using seven high quality case histories involving piles with diameters in the range 340mm to 4.2m. It is shown that the Unified method, adapted to enable estimation of the static resistance to driving (SRD), can lead to considerably improved predictions of driving resistance compared to an existing popular method used for SRD determination. Further refinements to the proposed formulation, referred to as UniSand-SRD, will be possible on examination of additional high quality case histories.

Keywords: Pile Driveability, Sand, Cone Penetration Test

1 INTRODUCTION

The selection of a suitable driving hammer is a key component of any driven piling project. The hammer needs to be capable of driving the pile to an embedded depth, determined from either static formulae or the measured dynamic resistance, without overstressing the pile material. The mobilisation of large hammers is expensive while delays caused by incorrect hammer selection is very costly, particularly in an offshore environment. Determination of the likely range of pile driving resistances for a given hammer is therefore critical.

Dynamic formulae used to assess driving resistance have now largely been replaced with more reliable numerical simulation techniques that are based on the wave equation. A key input to the accuracy of such simulations is the static resistance to driving (SRD) which is usually considered equivalent to the static axial capacity at the time of driving and excludes dynamic resistance components. The static capacity is assessed using static formulae that have been calibrated from static load tests conducted a number of days or weeks after pile installation. The static formulae can have a significant margin of error e.g. a coefficient of variation of measured to calculated static capacities of between 30 and 50% (e.g. Paikowsky et al. 2004, Dithinde et al. 2011).

The forthcoming 2022 version of the ISO-19901-4 guidelines replaces previously recommended methods for calculation of the static axial capacity of driven piles in sand with the 'Unified method' (Lehane et al. 2020). This method uses Cone Penetration Test (CPT) data to allow estimation of the static capacity of a driven pile in siliceous sand approximately 2 weeks after driving. The applicability of this method for determination of SRD is investigated in this paper. The 'Unified method' is first described and is then applied in a suitably modified format to predict the driving resistance of piles installed at a number of well characterised sites where detailed information concerning the hammer types and input energy were reported. Predictions are also obtained using the popular Alm & Hamre (2001) formulation for SRD (referred to in this paper as the *AH* method). Measured and predicted hammer blowcounts are compared and conclusions are drawn on the suitability of the modified format of the ISO-19901-4 'Unified method' and its performance relative to the AH method.

2 STATIC CAPACITY DETERMINED USING THE UNIFIED METHOD FOR PILES IN SAND

The Unified CPT-based method (ISO-19901-4, 2022) for driven piles in sand evolved from a Joint Industry Project (JIP) set up in 2013 to establish a database of high quality static load tests on driven piles that had the general consensus of a significant segment of the profession (Lehane et al. 2017). A subsequent JIP was established to develop a single CPT-based method for determination of static capacity that was calibrated using this 'Unified' database. This new method replaces the four CPT methods recommended in API/ISO (2011) for driven piles in silica sand, namely those referred to as Fugro-05 (Kolk et al. 2005), ICP-05 (Jardine et al. 2005), NGI-05 (Clausen et al. 2005) and UWA-05 (Lehane et al. 2005). The method and the database are referred to as 'Unified' as they were developed with input from authors of the four API/ISO (2011) methods.

A Unified method that allows estimation of the static post-consolidation capacity of driven piles in clay and silt has also been recently developed but is not discussed in this paper (*https://pile-capacity-uwa.com/*), Lehane et al. 2022a,b). Key elements of the Unified method for driven piles in sand are summarised here and full details are provided in Lehane et al. (2020, 2022a).

2.1 Coulomb Friction

In keeping with instrumented pile test data reported by Lehane et al. (1993), Chow (1997), Axelsson (2000), Lim (2015), and others, the peak external shaft friction (τ_f) is related to the radial effective stress at peak friction (σ'_{rf}) via Coulomb's law as (see Figure 1):

$$\tau_f = f_D\, \sigma'_{rf} \tan\delta_f = (\sigma'_{rc} + \Delta\sigma'_{rd}) \tan\delta_f$$
$$f_D = 1 \text{ in compression} \qquad (1)$$

where σ'_{rc} is the stationary (equalised) radial effective stress, $\Delta\sigma'_{rd}$ is the increase in radial effective stress during pile loading (attributed to dilation), δ_f is the constant volume sand-pile interface friction angle and f_D is a correction factor for the direction of axial loading (1.0 for compression loading and 0.75 under tension loading)

Load test data on equivalent instrumented piles tested in compression and tension (incl. data for piles in the Unified database and others reported by O'Neill 2001) indicate that τ_f developed in tension loading is consistently about 75% of the equivalent value of τ_f measured in compression tests. This is considered to be due to the Poisson ratio effect as the pile extends under tension loading (de Nicola and Randolph 1993) and due to the principal strain and stress axis reversals that take place between compressive pile driving and tension load testing, e.g. Lehane et al. (1993) and Galvis-Castro et al. (2019).

2.2 Stationary radial effective stress (σ'_{rc})

Tests on instrumented closed-ended piles have clearly demonstrated that the stationary radial effective stress (σ'_{rc}) follows a similar profile with depth as the CPT resistance (q_c) but that the σ'_{rc}/q_c ratio acting in any particular soil horizon reduces with increasing distance of that horizon from the pile tip (h) i.e.

$$\sigma'_{rc}/q_c = f(h) \text{ or } f(h/D) \qquad (2)$$

The correspondence between σ'_{rc} and q_c is consistent with the expectation that lateral stresses associated with insertion of a displacement pile vary with the cavity expansion limit stress and hence q_c (Randolph et al 1994). The dependence of σ'_{rc} on 'h' arises due to: (a) the reduction in stresses with increased distance from the concentrated focus of stress at the pile base and (b) increased level of (constrained) contraction of sand at the pile shaft as the number of shearing cycles imposed in any given soil horizon increases as the pile is driven deeper (White & Lehane 2004).

The Unified method assumes that, for a closed ended-pile, σ'_{rc} at any particular level varies with the distance from the pile tip normalised by the pile diameter (h/D). Justification for this normalisation are that (a) the geometric effect diminishes in proportion to the scale of the pile base (or diameter) and (b) the reduction in lateral stress due to contraction varies with the normal (cavity contraction) stiffness of the sand mass surrounding a pile, which varies inversely with the pile diameter. Further support for the use of the h/D term is provided in field and laboratory tests, such as those reported by Vesic (1970), Gregersen (1973), Robinsky et al. (1964) and others. These show that the average shaft shear stress in uniform sands remains 'quasi-constant' below a critical depth of a fixed multiple of the number of pile diameters (20 ±10D). In addition, Lehane et al. (2020) showed that the bias, with respect to D, in the Unified database of static load tests of the ratio of measured to calculated capacities (Q_m/Q_c) is removed when a h/D term is used instead of 'h' (as proposed by Alm & Hamre 2001).

2.3 Radial stress increase during pile loading ($\Delta\sigma'_{rd}$)

The restraint to dilation at the pile shaft during pile loading provided by the surrounding sand leads to an increase in radial stress on the pile shaft ($\Delta\sigma'_{rd}$) and hence an increase in peak shaft friction (τ_f); see Figure 1.

The value of $\Delta\sigma'_{rd}$ can be assessed from cavity expansion (CE) theory, where G is the operational shear modulus of the sand mass, D is the pile diameter, y is the dilation of the sand at the shaft interface, $2y/D$ is the cavity strain and k_n is the normal stiffness:

$$\Delta\sigma'_{rd} = 4G\, y/D = k_n\, y \qquad (3)$$

Data from constant normal stiffness (CNS) direct shear interface tests and tests on centrifuge piles with a range of diameters presented in Lehane et al. (2005) show that the cavity strains can be relatively large and,

contrary to assumption made in the UWA-05 and ICP-05 design methods (API 2011), the operational G value in Equation (3) is less than G_0 for typical pile diameters used in the field. The following approximate expression was deduced by Lehane et al. (2020) using $\Delta\sigma'_{rd}$ measurements on un-aged jacked piles and from parallel non-linear cavity expansion analyses:

$$\Delta\sigma'_{rd} = \left(\frac{q_c}{10}\right)\left(\frac{q_c}{\sigma'_v}\right)^{-0.33}\left(\frac{d_{CPT}}{D}\right) \quad (4)$$

where σ'_v is the vertical effective stress and d_{CPT} is the diameter of a standard 10cm^2 cone (35.7mm).

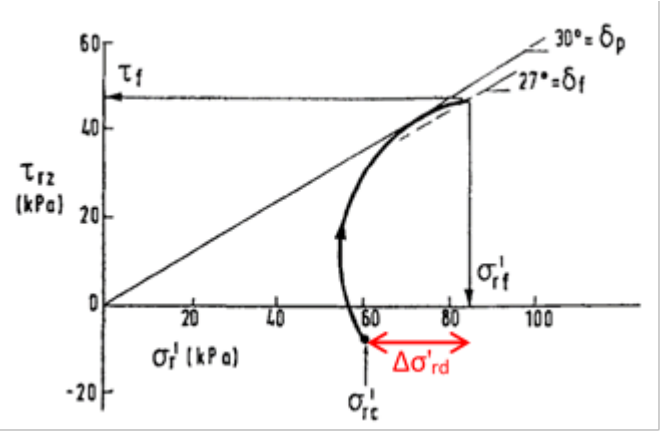

Figure 1. Typical variation of shear stress with radial effective stress during pile loading (Lehane 1992)

Most piles in the 'Unified database' have a diameter (D) between 350mm and 800mm. Equation (4) predicts that the increase in peak friction due to dilation (=$\Delta\sigma'_{rd}$ tanδ_f) for a 20m long pile in medium dense sand is about 35% for D=350mm but only 10% for D=800mm. The relative influence of dilation is clearly an important consideration when extrapolating from the smaller diameter database piles to larger diameter offshore piles. The predicted relative influence of dilation is also greatest in looser sands and for longer piles.

2.4 Allowance for partial plugging

Tests reported by Gavin & Lehane (2003), Paik et al. (2003), Igoe et al. (2011), and others, confirmed that τ_f varies with the degree of soil displacement imparted during installation and is largest for closed-ended or fully plugged piles and lowest for fully coring pipe piles. The average degree of soil displacement can be quantified using the effective area ratio, (A_{re}), which is the ratio of the volume of soil displaced ($V_{displaced}$) to the total pile volume (V):

$$A_{re} = V_{displaced}/V = 1 - PLR\,(D_i/D)^2 \quad (5)$$

The plug length ratio, PLR (defined as the plug length divided by embedded length, L_p/L) has been observed to vary primarily with the internal pile diameter (D_i). The following approximate expression was determined by Lehane et al. (2020) from a variety of field measurements and predicts PLR values of about 0.6 for D_i =200mm and 1.0 for D_i >1500mm:

$$PLR \approx \tanh\left[0.3\left(\frac{D_i}{d_{CPT}}\right)^{0.5}\right] \quad (6)$$

White et al. (2005) used a cavity expansion analogy to infer that the equalized lateral effective stress acting on the shaft of a driven pile (σ'_{rc}) should vary approximately with the effective area ratio (A_{re}) raised to a power of about 0.35. This analysis implies that Equation (2) can be extended to the following equation to cover all end conditions:

$$\sigma'_{rc}/q_c = f(\,h/D,\, A_{re}) \quad (7)$$

The most suitable form of Equation (7) cannot be determined from the limited number of available measurements of σ'_{rc} values on pipe piles. Therefore, in the calibration of the Unified method, Lehane et al. (2020) assumed that the h/D dependence of closed and open-ended piles is the same and that the reduced shaft friction developed on pipe piles can be accounted for approximately as a function of the effective area ratio.

2.5 Interface friction angle (δ_f)

It is clear that the shaft friction that can develop on a smooth pile is less than for a rough pile due to differences in respective interface friction angles (δ_f). Jardine et al. (1992), and others, have shown that δ_f reduces with increasing mean effective particle size (d_{50}) as the relative roughness increases. However, Yang et al. (2010), and others, have since shown that crushing of sand at the pile tip and subsequent extensive shearing during installation reduces the grading of all sands to that of a fine sand. As a consequence, the operational δ_f value for piles is insensitive to d_{50} and is 29 ±2.5° for typical pile roughnesses of both steel and concrete piles used in practice. A δ_f value of 29° was assumed in Equation (1) in the derivation of the Unified method.

2.6 Time effects

The shaft capacity of driven piles in silica sand increases with time over a period of least one year (e.g. Chow et al. 1998, Jardine et al. 2006, Karlsrud et al. 2014, Gavin et al. 2015). Such increases are not exhibited by bored piles and may be viewed as a recovery process following the 'trauma' of driven pile installation (Lim and Lehane 2014, Anusic et al. 2019). The new CPT method is calibrated using the Unified database comprising static load tests with a median equalisation period (or set-up time) of about two weeks. It is therefore likely to underestimate long-term capacities and over-estimate short-term capacities (including driving resistance).

The ratios of measured shaft capacities to those calculated using the Unified method (Q_s/Q_{uni}) for first-

time tension load tests performed on driven pipe piles at three sand sites are presented on Figure 2. The piles tested in the free-draining dense sands at Dunkirk and Blessington were 457 mm and 370mm diameter respectively (Jardine et al. 2006 and Gavin et al. 2013) while three pile diameters (89mm, 165mm and 450mm) were employed in medium dense sand in Shenton Park, Perth (Bittar et al. 2020a, Bittar 2022). It is seen that the

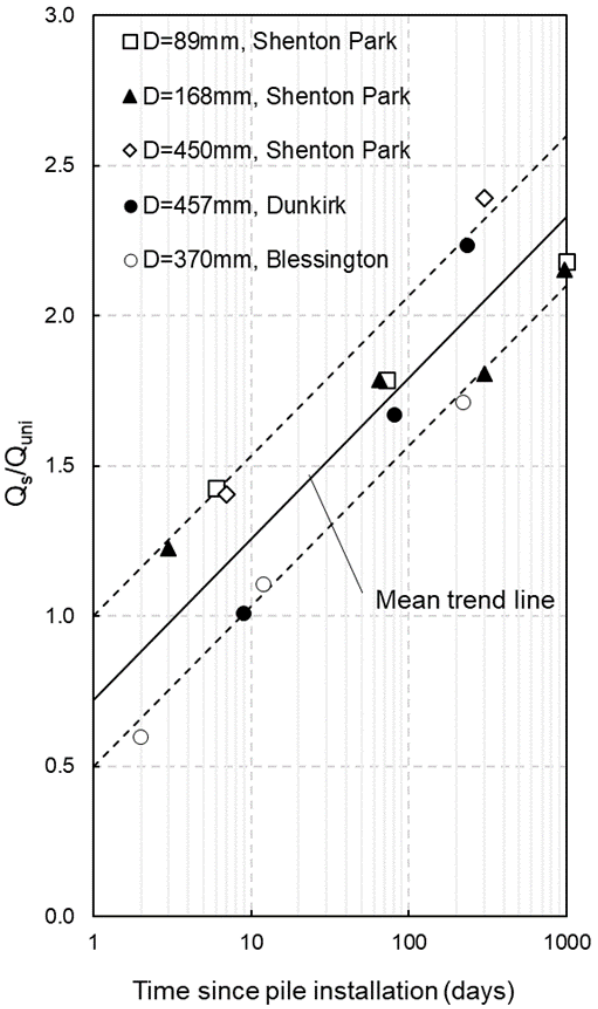

Figure 2 Variation of normalised shaft friction with set-up time in silica sand (Bittar 2022)

capacities measured around 2 weeks after installation (i.e. the set-up period assumed for the Unified method) are between 1.0 and 1.5 times the calculated capacity. This deviation is higher than typical but still within the expected margin of error of the method which calibration indicated has a coefficient of variation of measured to calculated capacities of 0.23.

Figure 2 highlights very significant ageing effects for all pile diameters and the equation of the mean variation of shaft friction (Q_s) with set-up time (t) is:

$$Q_s = Q_{uni}\,[0.7 + 0.54 \log t\ (\text{days})]$$

$$1\ \text{day} \leq t \geq 1000\ \text{days} \qquad (8)$$

The data indicate that long-term shaft capacities are likely to be at least double the capacity calculated using the Unified method (Q_{uni}). Data at short set-up times are limited but extrapolation of the mean trend line suggests that shaft friction mobilised during driving are unlikely to be greater than about 70% of Q_{uni}.

2.7 Base resistance

The Unified method allows assessment of the ultimate end bearing ($q_{b0.1}$) of a statically loaded pile. Under static loading, the plug remains stationary for piles with slenderness ratios (L/D) in excess of about 5 (Lehane & Randolph 2002). The value of $q_{b0.1}$, which acts over the full base area, increases with the degree of displacement imposed during the installation process (Gavin & Lehane 2003, Xu et al. 2008). The Unified method quantifies the degree of displacement using the effective area ratio (A_{re}), defined in equation (5). The degree of displacement is greatest for an end bearing pile or a pile that plugs during installation, and is a minimum for a fully coring or unplugged pile. Therefore, in accordance with equations (5) and (6), $q_{b0.1}$ can be expected to reduce with diameter with a minimum value at D ≥1.5m. The end bearing formulation of ICP-05 (Imperial College design method) incorporates this dependency indirectly by allowing $q_{b0.1}$ for pipe piles to reduce with pile diameter.

The equations proposed by the Unified method for the ultimate base resistance (Q_b) and base stress ($q_{b0.1}$) are as follows:

$$q_{b0.1} = [0.12 + 0.38A_{re}]q_p$$

$$Q_b = (\pi D^2/4)\ q_{b0.1} \qquad (9)$$

where q_p is an average value of q_c in the vicinity of the pile tip and, more specifically, is defined as the end bearing resistance expected for an 'imaginary cone' that has the same diameter as the pile being considered (or equivalent diameter for a pipe pile= $(A_{re}/\pi)^{0.5}$). The value of q_p is determined using a filter proposed by Boulanger and DeJong (2018) and its application in piling calculations is explained by Bittar et al. (2020b). Where pile tips extend a distance of about ten diameters into uniform sand deposits, the value of q_p may be taken as the average q_c value in the zone extending 1.5D above and below the pile tip.

2.8 Formulation summary: Unified method in sand

For convenience, the formulations for the Unified method are repeated in Equation (10) using the notation introduced earlier. This equation enables assessment of the static shaft capacity (Q_s) and base capacity (Q_b) of a driven pile in silica sand approximately 2 weeks after driving:

$$Q_s = \pi D \int^L \tau_f \, dz \quad (10a)$$

$$Q_b = q_{b0.1} (\pi D^2/4) \quad (10b)$$

$$\tau_f = f_D (\sigma'_{rc} + \Delta\sigma'_{rd}) \tan 29^o \quad (10c)$$

$$\sigma'_{rc} = (q_c/44) A_{re}^{0.3} [Max[1, h/D]]^{-0.4} \quad (10d)$$

$$\Delta\sigma'_{rd} = (q_c/10) (q_c/\sigma'_v)^{-0.33} (d_{CPT}/D) \quad (10e)$$

$$A_{re} = 1 - PLR (D_i/D)^2 \quad (10f)$$

$$PLR \simeq \tanh [0.3 (D_i/d_{CPT})^{0.5}] \quad (10g)$$

$$q_{b0.1} = [0.12 + 0.38 A_{re}] q_p \text{ or}$$
$$= [0.15 + 0.45 A_{re}] q_{c,Dutch} \text{ for } L/D > 5 \quad (10h)$$

$$q_{b0.1} = A_{re} \, q_{c,tip} \quad L/D \leq 5 \quad (10i)$$

$$f_D = 0.75 \text{ in tension, } 1.0 \text{ in compression} \quad (10j)$$

A plugged response under static loading is assumed for L/D >5. The value of q_p is determined using the procedure described Boulanger & De Jong (2018) and Bittar et al. (2020b). The value of $q_{c,Dutch}$ can be determined using a procedure described by Schmertmann (1978) and Xu et al. (2008).

3. ALM & HAMRE (2001) FORMULATIONS

3.1 External shaft friction

The Alm & Hamre (2001) formulations were developed from driveability studies conducted for piles in the North Sea and is a popular approach for determination of SRD. Driving resistance profiles predicted using this formulation are compared later in this paper with predictions using the SRD derived from the Unified method. The Alm & Hamre (AH) equations for shaft friction (Q_s) developed during pile driving are as follows:

$$Q_s = \pi d \int^L \tau_f \, dz \quad (11a)$$

$$\tau_{fmax} = K \sigma'_{v0} \tan \delta_f \quad (11b)$$

$$K = 0.0132 \, q_c (\sigma'_v/p_a)^{0.13}/\sigma'_{v0} \quad (11c)$$

$$\tau_{f,res} = 0.2 \, \tau_{fmax} \quad (11d)$$

$$\tau_f = \tau_{f,res} + [\tau_{fi} - \tau_{f,res}] \exp(- k \, h) \quad (11e)$$

$$k = (q_c/\sigma'_v)^{0.5}/80 \quad (11f)$$

where τ_{fmax} is the external friction developed at the pile tip, k determines the rate of degradation of τ_f with distance from the pile tip (h) and τ_{fres} is the lowerbound τ_f value.

It is of interest to compare the magnitudes of friction calculated using Equations (10) and (11). One such comparison is presented on Figure 3, which plots the (external) shaft friction calculated using the Unified method and *AH* formulations for the case of a 50m long, 2m diameter pipe pile with a wall thickness of 40mm in uniform medium dense and dense sand; this pile geometry is typical of what was used in calibration of the *AH* method from dynamic tests. It is evident that, although higher friction is predicted by *AH* close to the pile tip, the average shaft friction over the pile length is similar in magnitude to that calculated by the Unified method. This result is surprising given that the Unified method aims to predict shaft friction two weeks after driving (when some set-up has occurred) while *AH* predicts resistance at the time of driving. The reported inclusion in the *AH* method of the plug resistance (or internal friction) in the external friction formulation may explain the higher than expected τ_f values.

Further comparisons of both sets of shaft friction formulations indicated that the *AH* method predicts lower shaft resistance for smaller diameter pipe piles than the Unified method and also lower shaft friction for closed-ended piles compared with the Unified method.

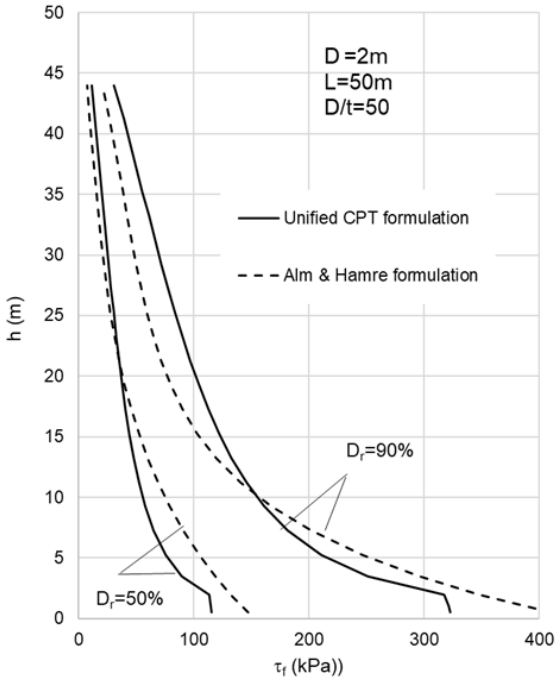

Figure 3 Comparison of profiles of τ_f given by Equations 10 and 11 for case wih D=2m, L=50m and D/t=50

3.1 Tip resistance

For pipe piles, internal friction is assumed in the *AH* method to be incorporated in the expression for external friction and the end resistance (Q_b) is derived as the product of the stress on the pile annulus (q_{ann}) and the annular area (where t is the pile wall thickness):

$$q_{ann} = 0.15 \, q_c (q_c/\sigma'_v)^{0.2} \quad (12a)$$

$$Q_b = q_{ann} (\pi D t) \quad (12b)$$

Equation (12) can be approximated as $q_{ann} = (0.3 \pm 0.05) \, q_c$ in medium dense and dense sand. For a typical D/t ratio of 50 (although this ratio is usually larger for typical monopiles), Equation 11b is equivalent to an

average base stress (acting over the full base area) of about $0.03q_c$.

The effective area ratio (A_{re}) of a large diameter offshore pile (for which the plug length ratio is unity) is equal to 0.08 for D/t ratio of 50. For this case, Equation (8) predicts an average ultimate base stress ($q_{b0.1}$) for the Unified method of $0.14q_c$ (where $q_p=q_c$ in uniform sands) for static loading. This proportion of q_c is almost five times that of the *AH* method, and reflects (i) the plugged end bearing response assumed in the Unified formula for static loading, (ii) lower degree of mobilisation of end bearing during a hammer blow compared with displacement of D/10 assumed by Unified method (noting *AH* was calibrated using dynamic testing) and (iii) the incorporation of a component of plug resistance in the AH formulation for external friction.

4. ADAPTING THE UNIFIED METHOD FOR SRD DETERMINATION

4.1 External shaft friction

The mechanisms governing the external shaft friction (Q_s) developed in a static load test are expected to be the same as those affecting the static resistance during driving (SRD). It may be assumed that the full friction needs to be overcome and that the external friction component of SRD is a multiple of the Q_s value determined from the Unified method. This multiple is likely to be about 0.7 or lower based on the observations discussed in relation to time effects on shaft friction (see Figure 2). A factor of 0.7 was employed in the computations presented in this paper.

4.2 Annular resistance for pipe piles

The pile penetration per blow during normal pile driving is typically between 10 and 30mm but often reduces to 2mm or less towards the end of driving. Using a twin-walled instrumented 660mm diameter pile with a wall thickness of 38mm, Han et al. (2020) showed that the stress mobilised on the annulus of a pipe pile (q_{ann}) was $0.72q_c$, $0.93q_c$ and $1.15q_c$ at respective pile base displacements of 33mm, 66mm and 149mm. These displacements equate to 5%, 10% and 22.5% of the pile diameter respectively and to 0.87, 1.7 and 3.9 times the wall thickness. Lehane & Gavin (2001) measured comparable annular stresses in model scale pile tests.

Han et al. (2020) also measured a residual base annular stresses after installation of approximately $0.15q_c$ and these measurements combined with their records of q_{ann} at larger displacements are presented on Figure 4. In the absence of any data on annular stresses at very low displacement, this figure also presents speculative relationships between q_{ann}/q_c and tip displacement (w_b) represented by the equation:

$$q_{ann}/q_c = (q_{ann}/q_c)_{residual} + \tanh\left[0.8(w_b/t)^{0.4}\right] \qquad (13)$$

Equation (13) leads to a q_{ann}/q_c value of about 0.4 at w_b= 2.5mm, which is a typical toe quake used in dynamic analyses.

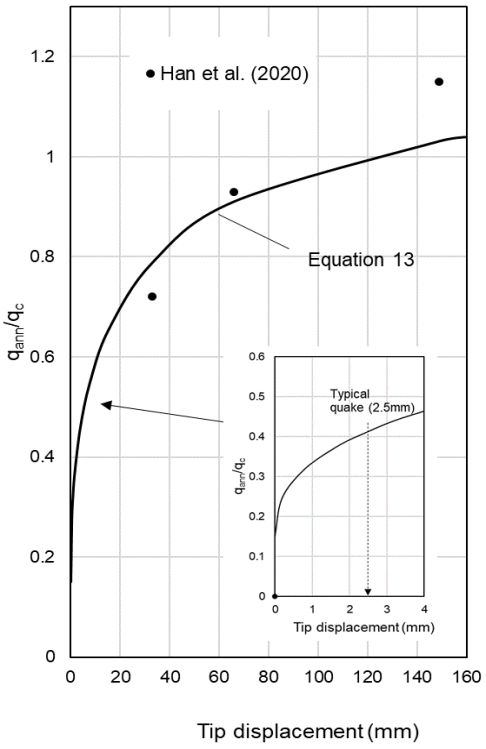

Figure 4 Projected normalised annular resistance variation with pile tip displacement

4.3 Internal shaft friction/plug resistance

The plug capacity is derived from internal friction in a pipe pile. While this capacity can be very significant under static loading (when the plug remains stationary), the inertia of the sand plug causes a phase shift between the accelerations in the pile wall and those in the interior of the plug during pile driving (Liyanapathirana et al. 1998). This phase shaft is such that pipe piles with a diameter greater than about 1.5m penetrate in a fully coring mode during driving (and those with a diameter greater than about 750mm have a plug length ratio (PLR) in excess of about 90%; see Equation 6). The plug capacity and internal friction can therefore be assumed to be negligible in the determination of SRD for larger diameter piles (D>750mm).

Partial plugging becomes significant when driving smaller diameter piles. Lehane & Gavin (2001) showed that the stress acting at the base of the plug (q_{plug}) is related directly to the incremental filling ratio or PLR and their data at plunging failure can, as shown on Figure 5, be represented by the following equation:

$$q_{plug}/q_c = \exp(-2 \times PLR) \text{ at plunging failure}$$
$$D < 750mm \qquad (14)$$

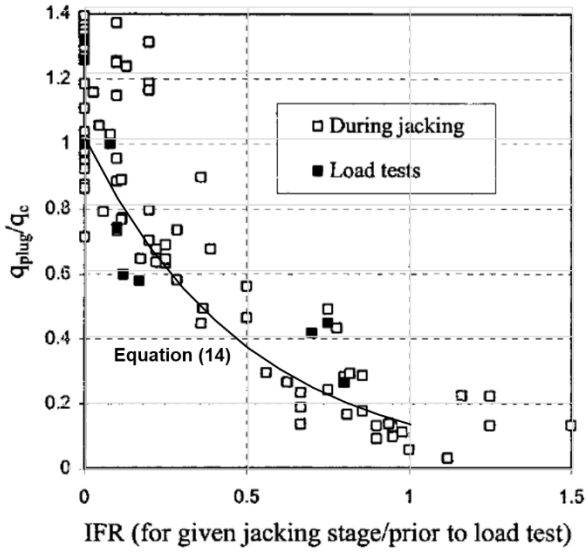

Figure 5 Normalised plug resistance at plunging failure as a function of filling ratio (Lehane & Gavin 2001)

Tentatively assuming 40% full mobilisation of both the plug and annular resistance (as inferred above at a quake of 2.5mm) gives the base load (Q_b) and the base stress during driving (q_b) acting over the full base area of (assuming $D_i \approx D$):

$$Q_b = 0.4\, q_{plug}\, \pi D_i^2/4 + 0.4\, q_c\, \pi D t \quad (15a)$$

$$q_b = Q_b/(\pi D^2/4) = 0.4\, q_c\, [\exp(-2\times PLR) + 4t/D] \quad (15b)$$

4.4 UniSand-SRD formulations for pipe piles

The term '*UniSand-SRD*' is used to distinguish the Unified method intended for static capacity estimation from the modified format for driving resistance assessment, discussed above. These equations for the SRD of a driven pipe pile (assuming a toe and shaft quake of 2.5mm) are summarised as follows:

$$Q_{s,SRD} = \pi D \int^L \tau_{f,SRD}\, dz \quad (16a)$$

$$Q_{b,\,SRD} = q_{b,SRD}\, (\pi D^2/4) \quad (16b)$$

$$\tau_{f,SRD} = 0.39\, (\sigma'_{rc} + \Delta\sigma'_{rd}) \quad (16c)$$

$$q_{b,SRD} = 0.4\, q_c\, [\exp(-2\times PLR) + 4t/D] \le 0.4 q_c \quad (16d)$$

$$\sigma'_{rc} = (q_c/44)\, A_{re}^{0.3}\, [Max(1, h/D)]^{-0.4} \quad (16e)$$

$$\Delta\sigma'_{rd} = (q_c/10)\, (q_c/\sigma'_v)^{-0.33}\, (d_{CPT}/D) \quad (16f)$$

$$PLR \simeq \tanh [0.3\, (D_i/d_{CPT})^{0.5}] \quad (16g)$$

5. PILE DRIVING CASE HISTORIES

5.1 Pile and site properties

Seven case histories involving driven pipe piles in sand with details summarised in Table 1 are examined in this paper. A more comprehensive study involving additional cases in a wider range of sand deposits and pile configurations is presently under preparation (Igoe et al. 2022).

All but one of seven piles considered were equipped with instrumentation during driving enabling the accurate measurement of the energy transferred to the piles (ENTHRU) to be inputted directly in the driveability analysis. An energy transfer efficiency of 80% was assumed for the single case (in Blessington) which did not obtain ENTHRU data. The case histories comprised driven pipe piles with diameters ranging by over one order of magnitude, from 340mm to 4.2m. The maximum pile embedment was 35m. The sands at the three North Sea sites considered (Shamrock, Cutter and Skiff sites) were typically medium dense and dense but also included relatively loose sand layers below 15m at both Shamrock and Cutter; full details including CPT profiles are available in Byrne et al. (2018). The sand at the other sites considered was dense with q_c typically ranging from 20 MPa to 30 MPa over the depths penetrated by the piles. More detail on these cases is provided in Igoe et al. (2022).

Table 1. Pipe pile driving case histories in sand.

Site	Shamrock	Cutter	Site A	Skiff
Pile Diameter (m)	4.2	4.2	2.0	0.76
Wall Thickness (mm)	50/60/70	50/60	38	38
Pile Length (m)	22	41	11.5	41
Penetration (m)	22*	29	10.5	34
Average ENTHRU (kJ) (from L/2 to L)	300±30	450±30	32 ± 5	50±20

Site	Blessington	Site B	Site C
Pile Diameter (m)	0.34	0.76	2.0
Wall Thickness (mm)	14	25	38
Pile Length (m)	7.3	7	11.5
Penetration (m)	7	6.1	10.5
Average ENTHRU (kJ) (from L/2 to L)	10 ± 1	11 ± 1	28 ± 3

*ENTHRU measurements only available to 22m

5.2 GRLWEAP analyses

The well-known GRLWEAP Offshore program (Pile Dynamics, 2010) was used to perform the predictions of the driving blowcount profiles (blows per 250mm) for the case histories considered. This program uses the wave equation to predict the pile response to each hammer blow to the pile (represented as a series of masses) where the soil resistance to the impact along the shaft is modelled by a series of springs and dashpots and the base resistance is represented by a single spring and dashpot below the pile tip. The static resistance along the shaft and base (SRD) is enhanced by additional resistance from viscous rate effects. A program default quake value (displacement to reach peak) of 2.5mm was

adopted for both the shaft and base while damping values of 0.25 s/m and 0.5 s/m were employed for the shaft and base respectively; these parameters are the same as those recommended by the *AH* method and are default values proposed for sand in GRLWEAP.

Shaft resistance varies with distance from the pile tip (h) in both the *UniSand-SRD* and *AH* methods meaning the input shaft friction distribution on a pile needs to be updated after each hammer blow. Schneider & Harmon (2010) show that such updating can be avoided with little loss in accuracy if the shaft resistance for every additional increment of penetration (ΔL) is set to τ_f^*, where

$$\tau_f^* = \frac{Q_{s,L} - Q_{s,L-\Delta L}}{\pi D \Delta L} \qquad (17)$$

where $Q_{s,L}$ and $Q_{s,L-\Delta L}$ are the shaft SRD values at depths of L and L-ΔL respectively determined using the Unified and AH formulations. Equation (17) was therefore used to input shaft resistance in the analyses.

5.3 GRLWEAP results

Measured profiles of blowcounts (per 250mm penetration) are compared on Figure 6 with profiles computed using the *UniSand-SRD* and *AH* formulations while a statistical summary comparing average measured and predicted blowcounts recorded for each 250mm penetration is provided in Table 2. Trends identified from Figure 6 and Table 2 are as follows:

Table 2. Comparison of predictive performance of UniSand-SRD and AH formulations for seven case histories considered

	UniSand-SRD		AH formulation	
	Average error in blowcounts per 250mm	Average % error in number of	Average error in blowcounts per 250mm	Average % error in number of blowcounts
Shamrock	18	27	16	24
Cutter	38	53	40	55
Site A	12	8	13	9
Skiff	16	22	27	37
Blessington	2	9	9	34
Site B	15	15	26	19
Site C	37	27	71	53
Euripides	10	20		
Average (all piles)	19	23	29	33
Average excl. Cutter	16	18	27	29

(i) Although predictions using *UniSand-SRD* and *AH* methods are generally in reasonable agreement with the measured profiles, both formulations lead to significant under-estimates of the blowcounts for the large diameter piles in the sand at Cutter (Figures 7e).

(ii) The blowcounts predicted by *UniSand-SRD* for piles excluding Cutter are in good agreement with the measured blowcounts and are, on average, within 16 hammer blows or 18% of the measured blowcount for each 250mm increment of penetration. This agreement is encouraging given the range of pile diameters and pile penetrations involved.

(iii) The exclusion of plug resistance in the *AH* formulation explains the strong under-prediction by this method for the small diameter pile at Blessington (D=0.34m); see Figure 7g. Other predictions by the *AH* method (apart from Cutter) give blowcounts that are typically about 25 to 30% larger than measured.

(iii) The predictions by the *UniSand-SRD* and *AH* methods in the medium dense sand at Cutter are, typically half of the measured blowcounts.

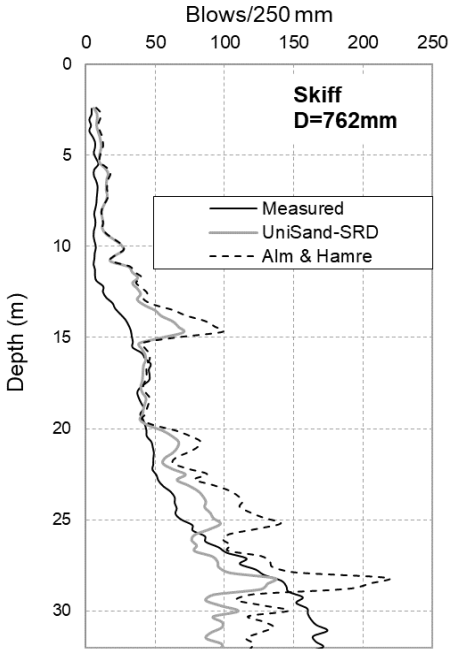

(a)

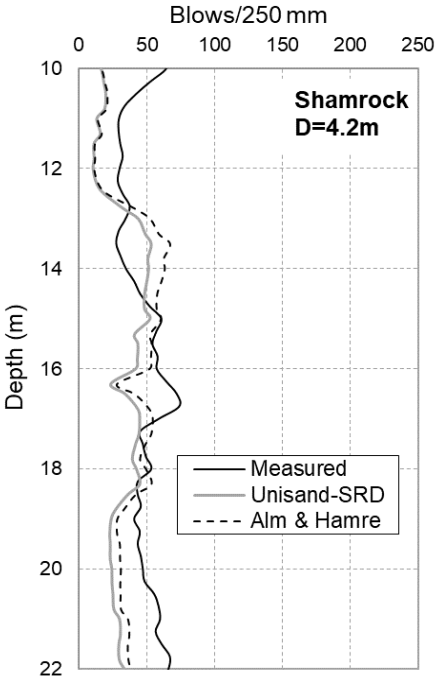

(b)

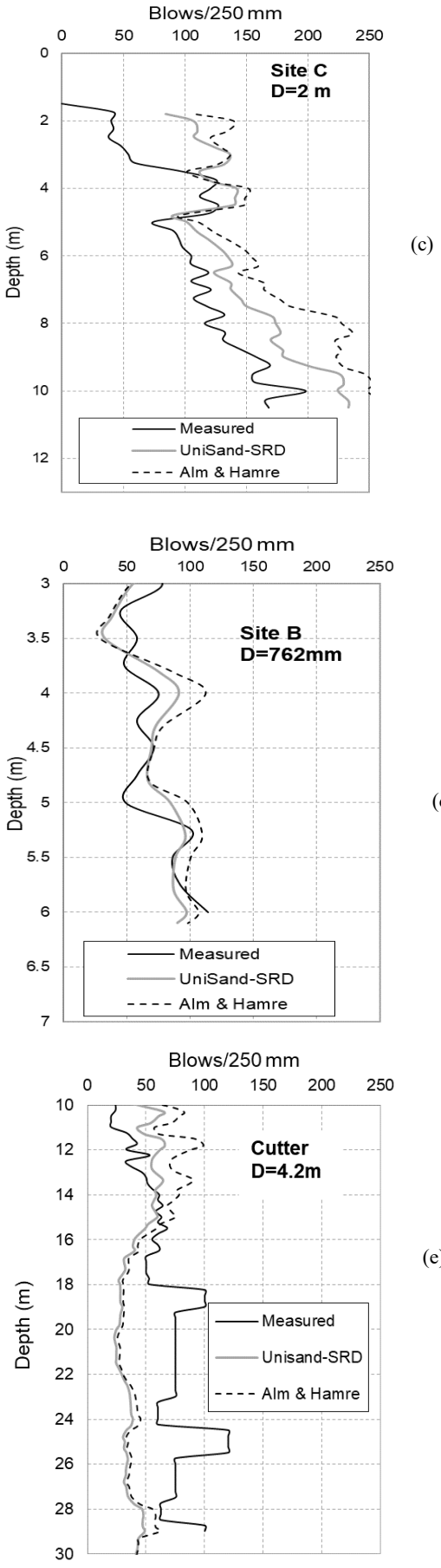

Figure 6 Measured and predicted blowcount profiles for seven case histories considered

Additional analyses revealed that increasing the annular resistance and overall base resistance of the Cutter piles led to a more jagged profile of blowcounts with depth that were not consistent with the trend of the measured blowcount profiles. It therefore appears that the discrepancy between measured and predicted blowcounts for this pile is due to under-estimation of shaft friction rather than that of base resistance. This underestimation may arise due to the presence of significant residual loads on these piles (Prendergast et al. 2020) or due to the need for specification of alternative quake and damping factors for the shaft and base from the default values employed. Further investigations (Igoe et al. 2022) indicate a tendency for

under-prediction of blowcounts during easy driving in loose and medium dense sands.

6. CONCLUSION

The formulations for the new 'Unified method' used for estimation of the static capacity of driven piles are used in this paper to develop the corresponding formulations to enable assessment of the static resistance to driving (SRD) of pipe piles in sand. These newly proposed formulations, referred to as *UniSand-SRD*, are tested against a small, but high quality, database of driving records assembled for pipe piles in sand. The results from wave equation driveability (GRLWEAP) analyses using the SRD determined from *UniSand-SRD* and the popular Alm & Hamre (2001) approach show that *UniSand-SRD* provides improved predictions of blowcount profiles with depth. Further refinements to the proposed formulation will be possible on examination of additional high quality case histories.

ACKNOWLEDGEMENTS

The authors would like to acknowledge the Norwegian Geotechnical Institute and all of the contributors and funding agencies that enabled the development of the Unified design formulations for driven piles.

REFERENCES

1) Alm T. and Hamre L. (2001). Soil model for pile driveability based on CPT interpretations. *Proc. 15th International Conference on Soil Mechanics and Foundation Engineering*, Istanbul, 1297-1302.

2) Anusic I., Lehane B.M., Eiksund G. and Liingaard M. (2019). Evaluation of installation effects on the set-up of field displacement piles in sand. *Canadian Geotechnical Journal*, 56(4), 461-472.

3) API (2011). ANSI/API RP 2GEO: Geotechnical and Foundation Design Considerations. ISO 19901-4:2003 (Modified), Petroleum and natural gas industries-Specific requirements for offshore structures, Part 4-Geotechnical and foundation design considerations. 1st edition. Washington, DC: API Publishing Services.

4) Bittar E. (2022). Design and optimisation of displacement piles for onshore and offshore applications. PhD Thesis, University of Western Australia.

5) Bittar E., Lehane B.M., Watson, P. and Deeks A. (2020a). Effect of cyclic history on the ageing of shaft friction of driven piles in sand. *Proc 4th Int. Symposium on Frontiers in Offshore Geotechnics*, ISFOG-4, Austin, Texas, 541-550.

6) Bittar E., Lehane B.M., Boulanger R.W. and DeJong J.T. (2020b). CPT filter to estimate the end bearing of closed-ended driven piles in layered sands. *Proc 4th Int. Symposium on Frontiers in Offshore Geotechnics*, ISFOG-4, Texas, 520-528.

7) Boulanger R.W.W. and DeJong J.T.T. (2018). Inverse filtering procedure to correct cone penetration data for thin-layer and transition effects. *Proc. 4th Int. Symposium on Cone Penetration Testing (CPT'18)*, Delft, The Netherlands.

8) Byrne T., Gavin, K., Prendergast L.J., Cachim, P., Doherty P. and Pulukul S.C. (2018). Performance of CPT-based methods to assess monopile driveability in North Sea sands. *Ocean Engineering*, 166, 76–91.

9) Chow F.C., Jardine R.J., Nauroy J.F., and Brucy F. (1998). Effects of Time on Capacity of Pipe Piles in Dense Marine Sand. *J. Geotech. and Geoenv. Engineering*, ASCE, 124, 254–264.

10) Clausen C. J. F., Aas P. M. & Karlsrud, K. (2005). Bearing capacity of driven piles in sand, the NGI approach. *Proc. 1st Int. Symp. on Frontiers in Offshore Geotechnics (ISFOG)*. Balkema, 574-580.

11) Dithinde, M., Phoon K.K., De Wet M. and Retief J.V. (2011). Characterization of Model Uncertainty in the Static Pile Design Formula. *J. Geotechnical and Geoenvironmental Engineering*, ASCE, 137 (1), 70-85.

12) Galvis-Castro A.C., Tovar-Valencia R.D., Salgado R., and Prezzi M. (2019). Effect of loading direction on the shaft resistance of jacked piles in dense sand. *Géotechnique*, 69(1)16–28.

13) Gavin K., Jardine R.J., Karlsrud K. and Lehane B.M. (2015). The effect of pile ageing on the shaft capacity of offshore piles in sand. Keynote paper. *Proc 3rd Int. Symposium on Frontiers in Offshore Geotechnics*, ISFOG-2, Oslo, 1, 129-152.

14) Gavin K.G. and Lehane B.M. (2003). Shaft friction for open-ended piles in sand. *Canadian Geotechnical J.*, 40(1), 36-45.

15) Gavin K.G., Igoe D.J.P. and Kirwan L. (2013). The effect of ageing on the axial capacity of piles in sand. *Proceedings of the Institution of Civil Engineers-Geotechnical Engineering* 166(2): 122-130.

16) Gregersen O.S., Aas G. and Dibiagio E. (1973). Load test on friction piles in loose sand. *Proc. 8th Int. Conf. on Soil Mech. Foundation Engng*: 109-117.

17) Han F., Ganju E., Prezzi M., Salgado R. and Zaheer M. (2020). Axial resistance of open-ended pipe pile driven in gravelly sand. *Géotechnique*, 70(2), 138–152.

18) Igoe, D. J. P., Gavin, K. G., & O'Kelly, B. C. (2011). Shaft capacity of open-ended piles in sand. Journal of Geotechnical and Geoenvironmental Engineering, 137(10), 903-913.

19) Igoe D.J.P., Lehane B.M. and Gavin K. G. (2022). Estimation of the driving resistance of piles in sand using the new ISO-19901-4 formulations for static capacity (in preparation).

20) Jardine, R. J., Chow, F. C., Overy, R. & Standing, J. R. (2005). *ICP design methods for driven piles in sands and clays.* Thomas Telford.

21) Jardine R.J, Standing J.R. and Chow F.C. (2006). Some observations of the effects of time on the capacity of piles driven in sand. *Géotechnique* 56(4): 227-244.

22) Jardine R.J., Lehane B.M. and Everton S. (1992). Friction coefficients for piles in sands and silts. *Proc. IV Conf. on Offshore site investigation and foundation behaviour*, Soc. for Underwater Technology, London, 661-677.

23) Karlsrud K., Jensen T.G, Wensaas-Lied E.K., Nowacki F and Simonsen AS. (2014). Significant Ageing Effects for Axially Loaded Piles in Sand and Clay Verified by New Field Load Tests. *Offshore Technology Conference*. Houston, Offshore Technology Conference.

24) Kolk H.J., Baaijens A.E. and Vergobbi, P. (2005). Results of axial load tests on pipe piles in very dense sands: The EURIPIDES JIP. *Proc. 1st Int. Symposium on Frontiers in Offshore Geomechanics*, ISFOG. Taylor & Francis, London. 661–667.

25) Lehane, B.M. (1992). Experimental investigations of pile behaviour using instrumented field piles. Imperial College London (University of London).

26) Lehane B.M. and Gavin K.G. (2001). The base resistance of jacked pipe piles in sand. *J. Geotechnical & Geoenvironmental Engrg.* ASCE, 127 (6), 473-480.

27) Lehane B.M. and Randolph M.F. (2002). Evaluation of a minimum base resistance for pipe piles in sand. *J. Geotechnical & Geoenvironmental Engrg.* ASCE, 128 (3), 198-205.

28) Lehane B.M., Jardine R.J., Bond A.J. and Frank, R. (1993). Mechanisms of shaft friction in sand from instrumented pile tests. *J. Geotechnical Engineering*, ASCE,119(1): 19–35.

29) Lehane B.M., Lim J.K., Carotenuto P., Nadim F., Lacasse S., Jardine R.J. and Van Dijk B. (2017). Characteristics of unified databases for driven piles. *Proc. 8th International Conf. Offshore investigation and Geotechnics: Smarter solutions for offshore developments*, Society for Underwater Technology, 1, 162-194.

30) Lehane B.M., Schneider J.A. and Xu X. (2005). The UWA-05 method for prediction of axial capacity of driven piles in sand. *Proc. Int. Symposium on Frontiers in Offshore Geotechnics*, Perth, 683-690.

31) Lehane B.M., Liu Z., Bittar E., Nadim F., Lacasse S., Jardine R.J., Carotenuto P., Jeanjean P., Rattley M., Gavin K., Gilbert R., Haavik J. and Morgan N. (2020). A new CPT-based axial pile capacity design method for driven piles in sand. *Proc 4th Int. Symposium on Frontiers in Offshore Geotechnics*, ISFOG-4, Texas, 463-477.

32) Lehane B.M., Liu Z., Bittar E., Nadim F., Lacasse S., Bozorgzadeh N., Jardine E., Ballard J-C, Carotenuto P., Gavin K., Gilbert R., Bergan-Haavik J., Jeanjean P. and Morgan N. (2022b). CPT-based axial capacity design method for driven piles in clay. *J. Geotech. & Geoenv. Engineering*, ASCE (in press)

33) Lehane B.M., Bittar E., Lacasse S., Liu Z. and Nadim F. (2022a). New CPT methods for evaluation of the axial capacity of driven piles. *Proc. 5th Int. Symp. On Penetration Testing*, CPT22, Bologne

34) Lim J.K. and Lehane B.M. (2014). Characterisation of the effects of time on the shaft friction of displacement piles in sand. *Géotechnique*, 64(6): 476–485.

35) Liyanapathirana D.S., Deeks A.J. and Randolph M.F. (1998). Numerical analysis of soil plug behaviour inside open-ended piles during driving, *Int. J. Num. & Anal. Methods in Geomechanics*, 22(4), 303-322.

36) O'Neill, M.W. (2001). Side Resistance in piles and drilled Shafts. *J. Geotechnical and Geoenvironmental Engineering*, 127(1): 3–16.

37) Paik K., Salgado R., Lee J. and Kim B. (2003). Behavior of open-and closed-ended piles driven into sands. *Journal of Geotechnical and Geoenvironmental Engineering* 129(4): 296-306.

38) Paikowsky S.G., Birgisson B., McVay M., Nguyen T., Kuo C., Baecher G., Ayyub B., Stenerssen K., O'Malley K, Chernauskas L. and O'Neill M. (2004). Load and resistance factor, Design (LFRD) for deep foundations. NCHRP Report 507, Transport Research Board, Washington D.C.

39) Pile Dynamics (2010). GRLWEAP Software.

40) Prendergast et al. (2020). Prendergast, L. J., Gandina, P., & Gavin, K. (2020). Factors influencing the prediction of pile driveability using CPT-based approaches. Energies, 13(12), 3128.

41) Randolph M.F., Dolwin J. and Beck R. (1994). Design of driven piles in sand. *Geotechnique*, 44(3), 427–448.

42) Robinsky et al. (1964)

43) Schneider J. and Harmon, I. (2010). Analyzing drivability of open ended piles in very dense sands. *J. Deep Found. Instit.*, 4, 32-44.

44) Schmertmann J.H. (1978). Guidelines for cone penetration test, performance and design. Report FHWA-TS-78-209, Washington, 145pp.

45) Vesic A.S. (1970). Tests on instrumented piles, Ogeechee River site. *Journal of Soil Mechanics & Foundations Div* 96(2), 561-584.

46) White D.J., Schneider J.A. and Lehane B.M. (2005). The influence of the pile end condition on the shaft capacity of displacement piles in sand. *Proc. 1st Int. Symposium on Frontiers in Offshore Geotechnics*, Perth, 741-748.

47) White D.J. and Lehane B.M. (2004). Friction fatigue on displacement piles in sand. *Geotechnique* 54(10), 645-658.

48) Xu X., Schneider J.A. and Lehane B.M. (2008). Cone penetration test (CPT) methods for end-bearing assessment of open- and closed-ended driven piles in siliceous sand. *Canadian Geotechnical Journal*, 45(1), 1130-1140.

49) Yang Z.X., Jardine R.J., Zhu B.T., Foray P. and Tsuha C.H.C. (2010). Sand grain crushing and interface shearing during displacement pile installation in sand. *Geotechnique*, 60(6), 469–482.